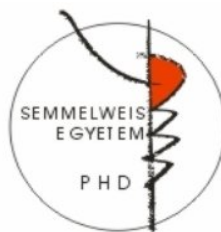


Influence of environmental distinctions on prooxidant properties of ascorbic acid and utilization of optical imaging tools for assessment

Ph.D. thesis - Short version

Pinar Avci

Doctoral School of Clinical Medicine
Semmelweis University



Supervisor: Norbert Wikonkal, MD, PhD, DSc

Official reviewers: Zsuzsanna Lengyel, MD, PhD

Miklós Csala, MD, PhD, DSc

President of the Final Examination Committee:

Miklós Kellermayer, MD, PhD, DSc

Members of the Final Examination Committee:

Gabriella Csík, PhD

Török László, MD, PhD

Budapest

2019

Introduction

There is already substantial evidence that ascorbic acid plays a major role in metabolic pathways and protects cells from the harmful effects of reactive species. Literature suggests that ascorbic acid, usually at high doses, can also exert selective toxicity against some tumor cells and infectious microorganisms, when specific conditions are met. Nevertheless, such prooxidant effects of pharmacologic ascorbic acid (P-Asc) remain controversial for various reasons such as fundamental differences between in vitro and in vivo conditions, lack of understanding of the exact mechanism of action and scarce clinical data that supports its efficacy. Additionally, specific conditions required for P-Asc to exert its anti-microbial and anti-cancer effects seem to vary depending on the tumor cell type and infectious agent.

C. albicans is a eukaryotic organism. As the member of a commensal microbiota, *C. albicans* can be isolated from the oral cavity, vaginal mucosa and gastrointestinal and urogenital tracts of most healthy individuals. However, as an opportunistic pathogen it is also the most common cause of fungal infections. *C. albicans* can efficiently adapt to a wide range of environmental conditions, by a rapid metabolic switch, which is usually accompanied by a phenotypic switch. One of the distinct features of *C. albicans* is its ability to grow in a number

of different morphological forms such as yeast, pseudohyphae and true hyphae. Like most microorganisms *C. albicans* also goes through different stages of growth such as lag phase, log phase and stationary phase in which it undergoes a variety of biochemical and morphological changes. Duration of each phase depends on various conditions such as temperature, pH, O₂ level and availability of nutrients. Although a few in vitro studies investigating P-Asc's prooxidant effects against *C. albicans* seem promising, results of in vivo studies suggest that P-Asc does not affect cell viability when used alone. Despite the great progress made in discovery of antifungal agents and candida biology, understanding the influence of in vitro culture conditions may provide better assessment of P-Asc's potential in vivo activity as well as its mechanism of action.

The most well accepted mechanism of action of P-Asc has been linked to its ability to generate H₂O₂ via Fenton reaction. Nevertheless, mechanisms for how H₂O₂ elicited by P-Asc, induces toxicity to cells are still under investigation. Some studies suggest that PARP activation through H₂O₂ induced DNA damage may lead to catabolization of NAD⁺, which would in turn deplete the substrate for NADH formation and hinder ATP synthesis. In the process of disposing H₂O₂ by an NADPH-dependent glutathione reductase/peroxidase system, NADPH is utilized to reduce GSSG back to GSH. In order to

replenish NADPH that is consumed during this process, some of the glucose that is used for glycolysis could be diverted to the pentose phosphate pathway that in turn would result in reduction of ATP. Another argument is that the degree of cytotoxicity depends on cellular proliferative activity, which is rather high in tumor cells as well as microorganisms that are in log phase of growth. These highly dividing cells usually have an increased rate of glucose uptake that parallels with higher expression of glucose transport channels. Dehydroascorbic acid, ascorbic acid's two-electron-oxidized form, is also transported by some of these channels, and its conversion increases intracellular levels of P-Asc by consuming cellular GSH and NADPH.

Basal cell carcinoma (BCC) is a keratinocyte-derived neoplasm of the skin. It is the most common type of cancer among Caucasians and its incidence is on the rise. BCC has various subtypes, based on in clinical presentation, growth pattern and histology. Growth pattern assists identification of aggressive and high-risk subtypes with potential tumor recurrence and, based on growth pattern BCC is classified as nodular, superficial, infiltrating, morpheiform, micronodular and basosquamous. Among these, nodular and superficial are considered as less aggressive and low risk subtypes. Recent literature suggests a close relationship between tumor cells and

their associated peritumoral stroma. A deeper understanding of the structural and molecular changes in peritumoral stroma enabled research groups to differentiate various tumor subtypes and assess tumor progression.

P-Asc, due to its reducing properties interferes with several conventional assays that rely on oxidation/reduction processes. Moreover, some fine changes of tissue pathology may not be apparent in standard histology sections. Further research exploiting new techniques which can allow imaging of both cellular and subcellular processes within living cells/tissues at the molecular as well as anatomic level could circumvent such limitations and help better assess P-Asc's prooxidant effects.

Objectives

Literature regarding P-Asc's prooxidant effects on tumor cells and infectious agents is seemingly controversial and, rather scarce for the latter. This controversy stems from various reasons including, but not limited to, differences in in vitro and in vivo conditions, tissue heterogeneity and AscH⁻'s tendency to interfere with reagents used in chemical assays. Moreover, its exact mechanism of action is yet to be further explored. In an attempt to clarify some of these problems, we aimed:

- 1/a.** To define specific metabolic and environmental conditions under which P-Asc exerts cytotoxic effects on *C. albicans* cells
- 1/b.** To investigate production of HO[•] formation and, indirectly the involvement of Fenton reaction in prooxidant effects of P-Asc on *C. albicans* cells
- 1/c.** To utilize lable free single live cell fluorescence imaging techniques to monitor intracellular redox status of P-Asc treated cells and real time treatment response
- 1/d.** To investigate morphologic and organelle specific alterations at the single cell level by utilization of lable free optical imaging tools
- 2.** To exploit lable free single live cell fluorescence imaging techniques to assess fine changes of tissue pathology during intravenous P-Asc (IVA) therapy that may not be apparent in standard hematoxylin and eosin stained histology sections.

Materials and methods

In vitro studies on *Candida albicans*

Materials

All chemicals used for the experiments were purchased from Sigma-Aldrich (MO, USA) unless otherwise stated. L-ascorbic acid was dissolved in phosphate-buffered saline (PBS) (free of $\text{Ca}^{2+}/\text{Mg}^{2+}$), PBS with D-(+)-glucose (20 g/l), YPD medium (yeast extract 10 g/l; peptone 20 g/l; dextrose 20 g/l, [BD-Difco™, NJ, USA]) or YPG medium (yeast extract 10 g/l; peptone 20 g/l [ForMedium Ltd., Norfolk, UK]; glycerol 38 g/l). Stock solutions of P-Asc were prepared on the same day of experiment and pH was adjusted to ≈ 7 with NaHCO_3 (Fisher Scientific, PA, USA). The final concentration of P-Asc was 90 mM in all experiments. Final concentrations of 2,2'-bipyridyl dissolved in dimethylacetamide and 2-[6-(4'-hydroxy)phenoxy-3H-xanthen-3-on-9-yl]benzoic acid [(3'-(p-Hydroxyphenyl)-fluorescein, HPF; Molecular Probes, OR, USA)] were 500 μM and 5 μM , respectively.

Cell culture

The *C. albicans* strain CEC 749 was used in this study. *C. albicans* was grown at 30°C on YPD agar and subcultured in liquid YPD medium in a rotary shaker incubator at rpm 120

(New Brunswick Scientific, NJ, USA), at 30°C. Log phase cultures obtained by reculturing stationary overnight cultures were used for all experiments except as follows: In one set of experiments, stationary cultures grown overnight or 4 days and a stationary culture grown for 4 days and then refreshed for 4 h were used. The reason for selecting two different time points for stationary phase cultures was because in some studies, *C. albicans* culture grown overnight or for 48 h was considered to be in stationary phase, while other studies reported the stationary phase to start much later, for example, between 3 and 8 days. All broth cultures were centrifuged at 3200 rpm for 10 min (centrifuge 5417 C; Eppendorf, Hamburg, Germany) and resuspended in PBS. The concentrations were then adjusted by measuring optical density (OD 570 of 0.65) to give an approximate cell density of 10^7 colony forming units (CFU)/ml. In one experiment, YPG medium and in another PBS with glucose, was used as described above.

Experimental design

The experiments were performed in 35×10 mm diameter Petri dishes (BD Falcon NJ, USA) containing approximately 3×10^7 cells in 3 ml growth media, PBS with glucose or PBS. To examine the effects of different media and glucose on P-Asc sensitivity, cells were compared in different growth media; YPD or YPG, or in PBS with glucose. YPD or YPG was used

both for initial growth and also for P-Asc treatment. Cells were agitated/shaken at 157 rpm at 37°C. At each time point two aliquots (10 µl each) were withdrawn. One was plated on YPD or YPG agar, the second was added to 90 µl PBS, then four additional tenfold dilutions were carried out in a 96 well plate. Subsequently, 10 µl was transferred from each well on agar plates via drop plate method. Plates were incubated between 24 and 48 h in an incubator at 30°C and cell viability was assessed by colony counting. In the next experiment cells were treated with P-Asc in PBS with agitation at 157 rpm (4 and 37°C); kept at 25 and 37°C under static condition (maintained unshaken for the duration of the experiment), or only in PBS with agitation at 157 rpm (4 and 37°C). Samples were withdrawn at different time points.

To determine whether the effect of P-Asc is dependent on the presence of iron, washed cells were resuspended in PBS solution with P-Asc, and 2,2'-bipyridyl, an iron chelator that predominantly binds Fe²⁺, was added at a final concentration of 500 µM. Subsequently, cells were incubated at 37°C with agitation at 157 rpm, and samples withdrawn at different time points.

Microscopy

Detection of hydroxyl radical generation

HPF fluorescent probe was added to washed cells and kept in a rotary shaker incubator with or without P-Asc in YPD or PBS or kept under static condition at 25°C with P-Asc in PBS. Subsequently, cells were spun down (3200 rpm, 3 min), supernatant was removed and they were resuspended in PBS. Images were acquired using a 35 mm 4-chamber glass-bottom petri dish (In Vitro Scientific, CA, USA).

HPF fluorescence images were captured by Olympus FV1000-MPE system with 40X NA0.8 water immersion lens. Fluorescence response of HPF was detected with single-photon excitation at 488 nm using multiline argon laser and the fluorescence emission were collected with laser scanning spectral detector at bandwidth 500–545 nm. Brightfield images were acquired simultaneously.

Assessment of intracellular redox status

Intracellular redox status was measured by autofluorescence imaging of NAD(P)H and FAD, using an Olympus FV1000-MPE confocal microscope system with 40X NA0.8 water immersion lens. The FAD autofluorescence was imaged with single-photon excitation at 488 nm using multiline argon laser and the autofluorescence was collected with laser scanning

spectral detector at bandwidth 500–600 nm. The autofluorescence of NAD(P)H was measured with two-photon excitation at 710 nm using MaiTai Deep See Ti:Sapphire laser (femtosecond) (Spectra-Physics, MaiTai HP DS-OL). The autofluorescence from two-photon excitation was collected with external two-channel photo-multiplier detector for NAD(P)H (band-pass filter 420–460 nm). Brightfield images were acquired simultaneously.

Transmission electron microscopy

C. albicans cells were spun down (3200 rpm, 3 min) immediately after treatment, supernatant was removed, cells were fixed in 2.5% glutaraldehyde and 2% paraformaldehyde, and stored overnight at 4°C. After spinning down (1200 rpm, 10 min) and decanting the fixative, 0.1 M sodium cacodylate buffer (pH 7.2) was added to the pellets. Following fixation, hot agar was added to each pellet. The solidified cell pellets were then processed routinely for transmission electron microscopy (TEM). The cell pellets were postfixed in 2% OsO₄ in sodium cacodylate, dehydrated in graded alcohol, embedded in Epon812 (Tousimis, MD, USA). Ultrathin sections were cut on a Reichert-Jung Ultracut E microtome (Vienna, Austria), collected on uncoated 200 mesh copper grids, stained with uranyl acetate and lead citrate, and examined on a Philips CM-10TEM (Eindhoven, The Netherlands) at 80 kV.

Ex-vivo studies on basal cell carcinoma

Treatment protocol

We have investigated skin biopsies taken from a 47 year old female patient who participated in a pilot study investigating the efficiency of long-term intravenous P-Asc (IVA) therapy on locally advanced basal cell carcinoma. This work was conducted at the Department of Dermatology, Venereology and Dermatoooncology of the Faculty of Medicine, Semmelweis University Budapest, Hungary, in accordance with the ethical standards as dictated by the Declaration of Helsinki and informed consent was obtained. Compounding of the intravenous vitamin C solution and its off-label use were approved by the Regional Committee of National Science and Research Ethics (TUKÉB 80/2010) and the National Institute for Quality and Organizational Development in Healthcare and Medicines (39.798/56/09). The infusion solutions were prepared from concentrated ascorbic acid solutions. Each 50 ml vial contained 25 g ascorbic acid (500 mg/ml) and pH was adjusted to 5,5-7 with sodium bicarbonate and edetate disodium. Solutions were diluted in 1000 ml Ringer's lactate infusion and administered for the duration of 3 hours by a Port-A-Cath device. In general IVA dosage was 1.8 g/kg body weight and it was administered for a total of 173 sessions.

Specimen collection and histopathology

Skin biopsy samples were taken from two different micronodular lesions after a two-week drug free interval, and subsequent two weeks of intensive (10 sessions) IVA therapy. Hematoxylin and eosin staining was performed on sections from 10% formalin-fixed and paraffin embedded skin biopsies.

Assessment of tumor collagen environment by second harmonic generation and two-photon excitation fluorescence microscopy

TPEFM and SHG images of deparaffinized tissue samples were acquired by a custom modified Axio Examiner LSM 7 MP laser scanning two-photon microscope (Carl Zeiss AG, Germany) using a 20X water immersion objective (W-Plan – APOCHROMAT 20x/1,0 DIC (UV) VIS-IR, Carl Zeiss AG, Germany). We employed a femtosecond pulse Ti-sapphire laser (FemtoRose 100TUN NoTouch, R & D Ultrafast Lasers Ltd, Hungary) tuned for a 800 nm excitation wavelength and a 395-415 nm band-pass emission filter to separate SHG signal from the TPEFM signal, which was collected at 565-610 nm and intracellularly attributed to mainly FAD. The size of each field of view corresponded to 0.42 x 0,42 mm, from which mosaic images of larger areas up to 6,72 x 6,72 mm were constructed by ImageJ software (NIH, USA). From the tumor nests and

their associated peritumoral stroma, five field of views were selected for quantitative analysis. Alterations in collagen morphology (fiber length and width) were assessed by CT-FIRE (v1.3) (LOCI, USA), a curvelet transform-fiber tracking algorithm in the selected field of views.

Conclusion

In order to address seemingly contradicting results from various studies investigating prooxidant effects of P-Asc and understand the conditions in which P-Asc shows antifungal activity against *C. albicans*, we have conducted our studies in different experimental settings and employed various optical imaging tools to assess its effects. According to our results, it is evident that some of the conflicting findings are due to the variations in cell metabolism and environment in vitro and in vivo conditions. P-Asc's efficacy as a prooxidant depends on oxygenation, temperature, access to nutrition, presence of iron and cell growth history. Therefore, inter- and intra-host heterogeneity in infections and, inter- and intra-tumor heterogeneity in cancer cells as well as their types should be taken into account while considering P-Asc as a prooxidant. Moreover, in the light of these findings, therapeutic response may be augmented by addition of vasoactive agents or hyperoxic gas mixtures. In an attempt to further elucidate mechanistic insights into P-Asc's prooxidant effects, we

employed various optical imaging modalities, some of which can potentially serve as real time monitoring tools for treatment response. To the best of our knowledge, we demonstrated for the first time that intracellular HO[•] generation by P-Asc is an active participant in oxidative damage to cells. Consistent with this finding, simultaneous label-free live cell imaging with TPEFM and conventional confocal microscopy revealed a marked reduction in NAD(P)H and elevation in FAD⁺ levels, respectively, the latter mainly in dying cells. Concomitantly, a vacuolar enlargement was captured by TEM, and coincided with the deflated ball appearance seen in brightfield microscopy.

Ex-vivo imaging studies were performed with TPEFM and SHG using limited number of skin biopsy samples taken from basal cell carcinoma lesions. Results indicated that IVA therapy alters tumor collagen environment. These novel label free optical imaging tools may enable real time in vivo evaluation of treatment response and eliminate biopsy as well as routine staining processes.

List of publications

Publications related to the thesis

Bánvölgyi A, Lőrincz K, Kiss N, **Avcı P**, Fésűs L, Szipőcs R, Krenács T, Gyöngyösi N, Wikonkál N, Kárpáti S, Németh K. Efficiency of long-term high-dose intravenous ascorbic acid therapy in locally advanced basal cell carcinoma – a pilot study. **Adv Dermatol Allergol.** 2019, in press, <https://doi.org/10.5114/ada.2019.83027> **IF: 1,47**

Avcı P, Freire F, Bánvölgyi A, Mylonakis E, Wikonkal NM, Hamblin M. Sodium ascorbate kills *Candida albicans* in vitro via iron-catalyzed Fenton reaction: importance of oxygenation and metabolism. **Future Microbiol.** 2016 Dec; 11(12): 1535–1547 **IF: 3,19**

Publications not related to the thesis

Aydogan BM, Aslan BC, Bilici S, Fasse J, **Avcı P**. Evaluation of ovarian reserve in women with psoriasis. **Gynecol Endocrinol.** 2019 Jan; 30:1-4 **IF: 1,45**

Yu C, **Avcı P**, Canteenwala T, Chiang LY, Chen BJ, Hamblin MR. Photodynamic Therapy with Hexa(sulfo-n-butyl)[60]Fullerene Against Sarcoma In Vitro and In Vivo. **J Nanosci Nanotechnol.** 2016 Jan; 16(1):171-81 **IF: 1,35**

Vecchio D, Gupta A, Huang L, Landi G, **Avci P**, Rodas A, Hamblin MR. Bacterial photodynamic inactivation mediated by methylene blue and red light is enhanced by synergistic effect of potassium iodide. **Antimicrob Agents Chemother**. 2015 Sep; 59(9):5203-12 **IF: 4,26**

Ferraresi C, Kaippert B, **Avci P**, Huang YY, de Sousa MV, Bagnato VS, Parizotto NA, Hamblin MR. Low-level laser (light) therapy increases mitochondrial membrane potential and ATP synthesis in C2C12 myotubes with a peak response at 3-6 h. **Photochem Photobiol**. 2015 Mar-Apr;91(2):411-6 **IF: 2,21**

Xia Y, Gupta GK, Castano AP, Mroz P, **Avci P**, Hamblin MR. CpG oligodeoxynucleotide as immune adjuvant enhances photodynamic therapy response in murine metastatic breast cancer. **J Biophotonics**. 2014 Nov;7(11-12):897-905 **IF: 3,77**

Yin R, Wang M, Huang YY, Huang HC, **Avci P**, Chiang LY, Hamblin MR. Photodynamic therapy with decacationic [60]fullerene monoadducts: effect of a light absorbing electron-donor antenna and micellar formulation. **Nanomedicine**. 2014 May;10(4):795-808 **IF: 5,01**

St Denis TG, Vecchio D, Zadlo A, Rineh A, Sadasivam M, **Avcı P**, Huang L, Kozinska A, Chandran R, Sarna T, Hamblin MR. Thiocyanate potentiates antimicrobial photodynamic therapy: in situ generation of the sulfur trioxide radical anion by singlet oxygen. **Free Radic Biol Med.** 2013 Dec; 65:800-810 **IF: 6,02**

Karimi M, **Avcı P**, Ahi M, Gazori T, Hamblin MR, Naderi-Manesh H. Evaluation of Chitosan-Tripolyphosphate Nanoparticles as a p-shRNA Delivery Vector: Formulation, Optimization and Cellular Uptake Study. **J Nanopharm Drug Deliv.** 2013 Sep;1(3):266-278

Karimi M, **Avcı P**, Mobasseri R, Hamblin MR, Naderi-Manesh H. The novel albumin-chitosan core-shell nanoparticles for gene delivery: preparation, optimization and cell uptake investigation. **J Nanopart Res.** 2013 Apr 1;15(4):1651 **IF:2,13**